Characterization of Ca^{2+}-Binding Sites in the Kidney Stone Inhibitor Glycoprotein Nephrocalcin Using Vanadyl Ions: Different Metal Binding Properties in Strong and Weak Inhibitor Proteins Revealed by EPR and ENDOR[†]

Devkumar Mustafi* and Yasushi Nakagawa

Department of Biochemistry and Molecular Biology, The University of Chicago, Cummings Life Science Center, 920 East 58th Street, Chicago, Illinois 60637

Received May 20, 1996; Revised Manuscript Received August 20, 1996[⊗]

ABSTRACT: Nephrocalcin (NC), a calcium-binding glycoprotein of 14 000 molecular weight as a monomer, is known to inhibit the growth of calcium oxalate monohydrate (COM) crystals in renal tubules. We have isolated NC from bovine kidney tissue and purified into four isoforms, fractions A−D. NC-A and NC-B strongly inhibit the growth of COM crystals, and NC-C and NC-D inhibit crystal growth weakly. The strong inhibitor proteins are abundant in normal subjects, whereas stone formers excrete less of NC-A and NC-B and more of NC-C and NC-D. NC-C was characterized with respect to its metal binding sites by using vanadyl ion (VO^{2+}) as a paramagnetic probe in electron paramagnetic resonance (EPR) and electron nuclear double resonance (ENDOR) spectroscopic studies. We demonstrated that VO^{2+} binds to NC-C with a stoichiometry of metal:protein binding of 4:1 and that VO^{2+} competes with Ca^{2+} in binding to NC-C. In NC-C, the metal ion is exposed to solvent water molecules and two water molecules are detected in the inner coordination sphere of the metal ion by ENDOR. In the metal binding environment of NC-A, as reported previously (Mustafi, D., & Nakagawa, Y. (1994) *Proc. Natl. Acad. Sci. U.S.A. 91*, 11323−11327), inner sphere coordinated water is completely excluded. Based on the results of the metal binding properties in both strong and weak inhibitor proteins, a probable mechanism of inhibition of COM crystal growth by NC has been outlined.

Nephrocalcin (NC[1]) is a calcium-binding glycoprotein of 14 000 molecular weight as a monomer. It inhibits growth of calcium oxalate monohydrate (COM[1]) crystals in renal tubules (Nakagawa et al., 1983). NC has been isolated in four isoforms from urine of normal subjects (Nakagawa et al., 1983) and kidney stone patients (Nakagawa et al., 1985a), from surgically removed calcium oxalate kidney stones (Nakagawa et al., 1987), and from kidney tissue of nine species of vertebrates (Nakagawa et al., 1991). Purification of NC from bovine kidney tissue by DEAE-cellulose chromatography showed that it also consists of four isoforms which have been designated as fractions A−D (Nakagawa et al., 1984, 1985b, 1987). NC fractions A−D were also obtained similarly from other species as described earlier (Nakagawa et al., 1983, 1985a). Fractions A and B of NC, the "strong" inhibitor proteins, are abundant in normal subjects (Nakagawa et al., 1983) while stone formers excrete less of NC-A and NC-B and more of "weak" inhibitor proteins NC-C and NC-D (Nakagawa et al., 1985a). NC is an acidic glycoprotein containing 33% acidic amino acid residues (Asp and Glu) and about 5% each of aromatic and basic amino acid residues (Nakagawa et al., 1985b). Fractions A−D differ according to the content of carbohydrate and phosphate. Also, the "strong" inhibitor proteins contain 3 equiv of γ-carboxyglutamic acid (Gla) residues per NC molecule. Gla residues are not found in NC of stone-forming patients (Nakagawa et al., 1985b).

It has been shown that normal urine is supersaturated with respect to calcium oxalate (Nancollas, 1979). Robertson et al. (1969) made an important observation concerning the growth of calcium oxalate crystals. By examining COM crystals in fresh warm urine at 37 °C, they found that only stone formers have large and aggregated crystals, while normal subjects have very small COM crystals (Robertson et al., 1969). Therefore, the strong inhibitor proteins must have unique properties that prevent growth, aggregation, and secondary nucleation of COM crystals. The dissociation constant for weak inhibitor proteins for binding Ca^{2+} or COM crystals is about 2 orders of magnitude higher than that of the strong inhibitor proteins (Nakagawa et al., 1983, 1985a). The metal binding properties of different fractions of NC characterized as strong and weak inhibitor proteins may be responsible for differences in the extent of their ability to inhibit COM crystal growth.

Here we report the metal binding properties and their environments in NC-A and NC-C and relate them to different functional properties in inhibiting COM crystal growth by strong and weak inhibitor proteins. We have previously characterized the metal binding properties of NC-A by electron paramagnetic resonance (EPR) and electron nuclear double resonance (ENDOR) spectroscopic studies using the vanadyl ion (VO^{2+}) as a paramagnetic probe (Mustafi & Nakagawa, 1994). The VO^{2+} ion has been shown to be an

[†] This work was supported by a grant from the National Science Foundation (MCB-9513538).

* Author to whom correspondence should be addressed. Telephone: (773)702-1667. FAX: (773)702-0439. E-mail: Mustafi@biovax.uchicago.edu.

[⊗] Abstract published in *Advance ACS Abstracts*, November 1, 1996.

[1] Abbreviations: CD, circular dichroism; COM, calcium oxalate monohydrate; EPR, electron paramagnetic resonance; ENDOR, electron nuclear double resonance; Gla, γ-carboxyglutamic acid; hf, hyperfine; hfc, hyperfine coupling; NC, nephrocalcin; NC-A, NC-B, NC-C, and NC-D correspond to isoforms A, B, C, and D of nephrocalcin, respectively; PIPES, piperazine-*N*,*N*′-bis(2-ethanesulfonic acid); rf, radiofrequency.

S0006-2960(96)01200-7 CCC: $12.00

effective paramagnetic substitute for many divalent metal ions in metalloproteins and metalloenzymes (DeKoch et al., 1974; Chasteen, 1981, 1983; Chasteen et al., 1973) and is, in particular, an effective substitute for Ca^{2+} and Mg^{2+} (Ahmed et al., 1987; Mustafi et al., 1992; Mustafi & Nakagawa, 1994). VO^{2+} is an ideal substitute for Ca^{2+} because its electrostatic energy term (Z/r) is similar to that of Ca^{2+} (Williams, 1985) and, like Ca^{2+}, VO^{2+} has a high affinity for binding to oxygen-donor ligands (Chasteen, 1981). In this study we characterized the metal binding properties of NC-C using circular dichroism (CD), EPR, and ENDOR methods using VO^{2+} ions. We have shown that VO^{2+} binds to NC-C with a stoichiometry of metal:protein binding of 4:1. Furthermore, we have also demonstrated that VO^{2+} competes with Ca^{2+} in binding to NC-C, similar to that of NC-A (Mustafi & Nakagawa, 1994). CD studies revealed that conformational properties of the protein secondary structure are different in NC-A and NC-C upon introduction of the native Ca^{2+} or VO^{2+} ions. Furthermore, the results of EPR and ENDOR studies of VO^{2+} complexed to NC-A and NC-C clearly indicate that the metal binding environments in strong and weak inhibitor proteins are different. In NC-C, the metal ion is exposed to solvent water molecules and two water molecules are detected by ENDOR in the inner coordination sphere of the metal ion. On the other hand, in the metal binding environment of NC-A, the coordinating ligands to the metal ions were only from the protein residues with complete exclusion of solvent water from the inner coordination sphere (Mustafi & Nakagawa, 1994).

EXPERIMENTAL PROCEDURES

Materials

NC was isolated from fresh bovine kidney tissue (Brown Packing Co., S. Holland, IL) and separated into four fractions by DEAE-cellulose chromatography (Whatman DE-52), as described previously (Nakagawa et al., 1983). These fractions were eluted by using a linear gradient of NaCl from 0.1 to 0.5 M in 0.05 M Tris-HCl at pH 7.3 and collected at the following ionic strengths: NC-A at 10−15 mS, NC-B at 16−23 mS, NC-C at 24−27 mS, and NC-D at 32−38 mS. Fraction C of NC (NC-C) which exhibits much lower affinity for Ca^{2+} binding compared to NC-A, was used in this study. NC-C serves as a model for NC from patients with stone-forming tendencies (Nakagawa et al., 1983, 1985a, 1991) and can be used as a model system for a weak inhibitor protein. NC-C was eluted at a conductivity between 24 and 27 mS and then further purified by Sephacryl S-200 gel filtration chromatography (Pharmacia-LKB, 2 × 100 cm) using 0.05 M Tris-HCl buffer at pH 7.3 containing 0.2 M NaCl and 0.02% sodium azide. Figure 1 illustrates chromatograms of homogeneous preparations of NC-A and NC-C. In this procedure, using 738 g of bovine kidney we have typically isolated 99 mg of purified NC-A and 27 mg of purified NC-C. Chromatographically purified NC-C was dialyzed and lyophilized and then dissolved in 0.03 M PIPES at pH 5.8 to a concentration of 12−14 mg/mL for spectroscopic studies. This solution was then treated with Chelex-100 by dialysis to ensure removal of metal ions. Metal ion removal (mostly Ca^{2+}) was confirmed by atomic absorption (Nakagawa et al., 1983).

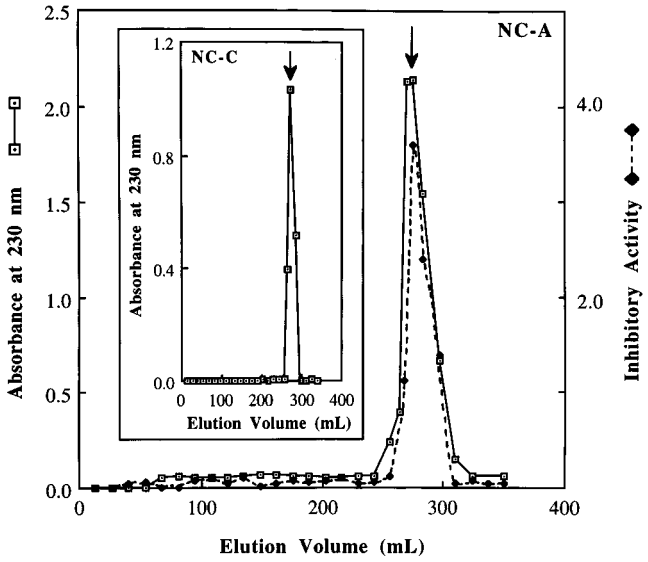

FIGURE 1: Rechromatography of NC-A and NC-C (in the inset) using a Sephacryl S-200 column (2 × 110 cm) and using 0.05 M Tris-HCl buffer (pH 7.3) containing 0.2 M NaCl and 0.02% NaN_3. For NC-A, the inhibitory activity, measured by [^{14}C]oxalate incorporation method using COM as seed crystals (Nakagawa et al., 1983, 1987), is also shown in the figure. First four isoforms were separated using a linear NaCl gradient (Nakagawa et al., 1983), and then fractions A and C of NC were rechromatographed. As indicated by arrows, the molecular weight of the peak in both NC-A and NC-C was estimated to be 14 000 by gel filtration chromatography and SDS PAGE (Nakagawa et al., 1983).

Methods

Chemical Analyses. Protein concentration was determined by alkaline hydrolysis followed by the ninhydrin color reaction at 570 nm (Nakagawa et al., 1983) using bovine serum albumin as a calibration standard. Phosphate content was determined by the modified Fiske−Subbarow method after ashing and hydrolysis (Ames, 1966). Carbohydrate analysis was accomplished by gas chromatography after hydrolysis in 1 N HCl−methanol at 80 °C for 24 h followed by neutralization and trimethylsilylation (Clamp et al., 1971).

Molecular weight, 14 000 as a monomer, was estimated from the elution profile of Sephacryl S-200 column chromatography calibrated with bovine serum albumin (68 kDa), carbonic anhydrase (29 kDa), soybean trypsin inhibitor (21 kDa), and lysozyme (14 kDa).

Circular Dichroism. CD spectra of NC-C in the absence or presence of VO^{2+} and Ca^{2+} ions were recorded with a JASCO J-600 CD spectropolarimeter. NC-C was diluted to 0.20 mg/mL of protein using 0.03 M PIPES at pH 5.8. The protein solution was then titrated with $CaCl_2$ or freshly prepared $VOSO_4$ solution to the desired ratio of [VO^{2+}]:[NC-C] or [Ca^{2+}]:[NC-C]. CD spectra in the far-ultraviolet region were measured for samples using a 1 mm light path length and were the average of three spectral scans. For the calculation of molar ellipticity [θ], a mean residue weight of 110 was used. The CD spectra were calibrated using an aqueous solution containing 0.06% (1*S*)-(+)-10-camphorsulfonic acid.

EPR and ENDOR. Vanadyl−nephrocalcin complexes were prepared by mixing together the desired quantity of NC-C (or NC-A) in 0.03 M PIPES buffer at pH 5.8 with

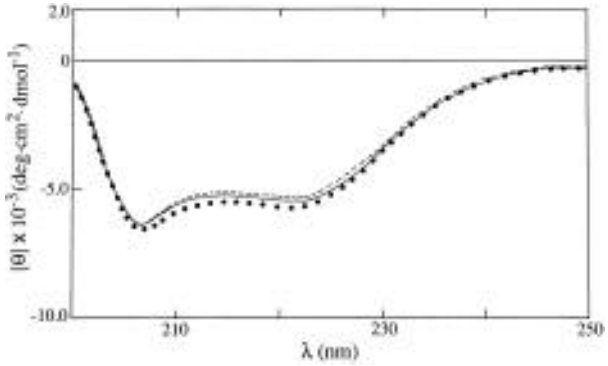

FIGURE 2: CD spectra of metal-free NC-C and NC-C complexed to VO^{2+} and Ca^{2+} ions. The spectra are shown for the following samples: metal-free NC-C, indicated by the dotted line; [VO^{2+}]:[NC-C] molar ratio of 4:1, indicated by the solid line; and [Ca^{2+}]:[NC-C] molar ratio of 4:1, indicated by the dashed line. NC-C was diluted to 0.20 mg/mL of protein in 0.03 M PIPES buffer at pH 5.8. The protein was then titrated with $CaCl_2$ or freshly prepared $VOSO_4$ solutions to the desired ratio of metal:NC-C.

$VOSO_4$ in a small quantity of H_2O or D_2O. VO^{2+} was added under a nitrogen atmosphere. For EPR and ENDOR studies, the final concentration of NC was about 1 mM while the metal ion concentration varied from 0 to 10 mM. All solutions were purged with nitrogen gas and stored frozen in EPR sample tubes to prevent oxidation.

EPR and ENDOR spectra were recorded with use of an X-band Bruker ESP 300E spectrometer equipped with an Oxford Instruments ESR 910 liquid helium cryostat and Bruker digital ENDOR accessories, as previously described (Mustafi & Nakagawa, 1994; Mustafi & Makinen, 1995). The ESP 300E spectrometer is equipped with a complete computer interface (ESP 3220 data system) for spectrometer control, data acquisition and processing, and communications. Typical experimental conditions for EPR measurements: sample temperature, 20 K; microwave frequency, 9.45 GHz; incident microwave power, 64 μW (full power, 640 mW at 0 dB); modulation frequency, 12.5 kHz; and modulation amplitude, 0.8 G. Typical experimental conditions for ENDOR measurements: microwave power, 6.4 mW; rf power, 50−70 W; rf modulation frequency, 12.5 kHz; and rf modulation depth, 10−20 kHz. The static laboratory magnetic field was not modulated for ENDOR.

RESULTS

Conformational Properties of Nephrocalcin-C

Since we have employed the VO^{2+} ion as a paramagnetic substitute for Ca^{2+} in binding to the native protein, it was necessary to determine whether substitution of Ca^{2+} by VO^{2+} in NC-C induces structural or conformational alterations different from those induced by Ca^{2+} binding. Figure 2 illustrates the CD spectra of metal-free NC-C and of Ca^{2+}- and VO^{2+}-saturated NC-C. As illustrated in Figure 2, CD spectra of metal-free NC-C and NC-C bound to either VO^{2+} or Ca^{2+} ions are nearly identical, indicating no conformational change of the protein secondary structure induced by either metal ion. These results are different from those of NC-A where changes in the secondary structure are observed upon binding with either VO^{2+} or Ca^{2+} ions (Mustafi & Nakagawa, 1994).

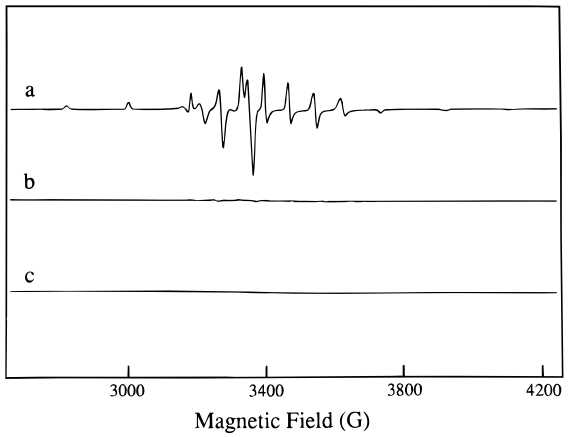

FIGURE 3: First-derivative EPR spectra of the VO^{2+} complexes in frozen aqueous solution: (a) [VO^{2+}]:[NC-C] molar ratio of 4:1; (b) [VO^{2+}]:[Ca^{2+}-saturated NC-C] molar ratio of 4:1; and (c) VO^{2+} in buffer. The final concentration of NC-C of 7.46×10^{-4} M in PIPES buffer at pH 5.8 was used.

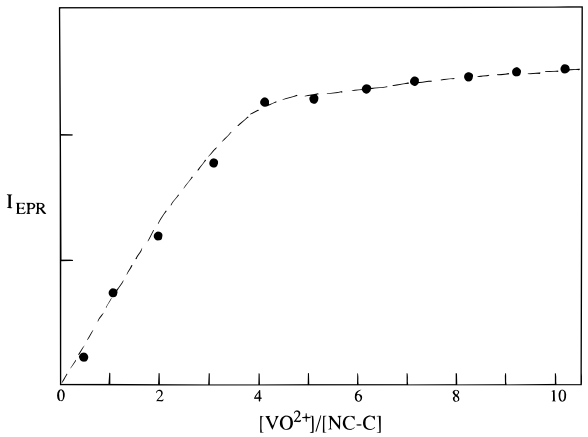

FIGURE 4: EPR spectrometric titration of the VO^{2+} ion complexed to NC-C. The EPR signal intensities of the $-3/2$ perpendicular line of VO^{2+} are plotted as a function of [VO^{2+}]:[NC-C] ratio. The final concentration of NC-C of 6.12×10^{-4} M in PIPES buffer at pH 5.8 was used. Dashed lines are drawn through the experimental points.

EPR of VO^{2+}−NC-C: Stoichiometry of Vanadyl−Nephrocalcin Binding

In the V^{4+} ion with a $3d^1$ configuration, the unpaired electron is strongly coupled to the ($I = 7/2$) ^{51}V nucleus. In frozen solution, the VO^{2+} ion is characterized by an axially symmetric **g** matrix and exhibits eight parallel and eight perpendicular absorption lines (Kivelson & Lee, 1964; Albanese & Chasteen, 1978). Figure 3 illustrates the EPR spectra of VO^{2+}−NC-C complexes. Since in the pH 5−11 region VO^{2+} forms an EPR-silent, polymeric $VO(OH)_2$ species (Francavilla & Chasteen, 1975), the peak-to-peak amplitude is proportional only to the amount of NC-C-bound VO^{2+}. An increase in signal amplitude was observed up to a [VO^{2+}]:[NC-C] molar ratio of 4:1. Moreover, when VO^{2+} was added to Ca^{2+}-saturated NC-C, the trace was similar to that of VO^{2+} in buffer alone, indicating that VO^{2+} is bound only at the same sites as Ca^{2+}. This is illustrated in Figure 3.

Figure 4 illustrates a plot of the peak-to-peak amplitude of the $-3/2$ perpendicular EPR feature as a function of the [VO^{2+}]:[NC-C] ratio. The $-3/2$ perpendicular resonance feature was selected to monitor the stoichiometry of VO^{2+}

Table 1: Comparison of EPR Parameters[a] of VO^{2+} Complexes

complex[b]	$g_{\|}$	$g_{\perp}$	$A_{\|}$	$A_{\perp}$	ref[c]
$[VO^{2+}-$NC-C]	1.937	1.982	539.0	205.9	this work
$[VO^{2+}-$NC-A]	1.940	1.989	535.4	193.5	1
$[VO(H_2O)_5]^{2+}$	1.933	1.978	547.4	211.9	2
$[VO(acac)_2]$ in THF	1.945	1.981	506.7	183.3	3
[VO(TPP)] in THF	1.964	1.989	477.0	162.4	3
$[VO(S_2O_2)]$[d]	1.969	1.979	443.5	184.6	4

[a] Hyperfine values are given in units of MHz. [b] acac, acetylacetonate; THF, tetrahydrofuran; TPP, tetraphenylporphyrin. [c] References: 1, Mustafi & Nakagawa, 1994; 2, Albanese & Chasteen, 1978; 3, Kivelson & Lee, 1964; 4, Chasteen, 1981. [d] Extracted from ref 4 (Chasteen, 1981) for VO^{2+} complexes with two oxygen-donor and two sulfur-donor ligands in the equatorial plane.

binding since it has virtually no overlap with nearby parallel EPR transitions. Figure 4 shows an increase in signal intensity up to a $[VO^{2+}]$:[NC-C] ratio of 4:1, after which the signal intensity remains virtually constant, indicating that the stoichiometry of VO^{2+} binding to NC-C is 4:1. A similar conclusion concerning the stoichiometry of VO^{2+} binding to NC-A was drawn on the basis of CD and EPR studies of VO^{2+}-reconstituted NC-A (Mustafi & Nakagawa, 1994). Also, the stoichiometry of Ca^{2+} binding to NC-A was drawn on the basis of ^{31}P NMR studies of $Ca^{2+}-$NC-A complexes and on the basis of equilibrium dialysis of the native NC-A with ^{45}Ca (Nakagawa et al., 1985b).

Coordination Environment of VO^{2+} Ion in Nephrocalcin-C

To identify the origin of the metal coordinating ligands in the $VO^{2+}-$NC-C complex, we have carried out both EPR and ENDOR studies. The principal hyperfine values $A_{\|}$ and $A_{\perp}$ for the vanadium nucleus and the values of $g_{\|}$ and $g_{\perp}$ reflect the environment of the metal ion in the vanadyl complexes (Chasteen, 1981). Since $g_{\|}$ and $A_{\|}$ depend primarily on the donor-ligand atoms in the equatorial plane of the VO^{2+} ion, the values of $g_{\|}$ and $A_{\|}$ are the most useful guide for comparing different environments (Chasteen, 1981). In Table 1, we compare EPR parameters of VO^{2+} complexes of NC-C and NC-A to those of other VO^{2+} complexes containing oxygen, nitrogen, and sulfur ligands in the equatorial plane. The results show that the EPR parameters of $VO^{2+}-$NC-C complexes are similar to those of VO^{2+} complexes with oxygen-donor ligands in the equatorial plane.

Changes in EPR line widths can also be analyzed to yield information about the symmetry and coordination environment of a VO^{2+} ion (Albanese & Chasteen, 1978). For the $[VO(H_2O)_5]^{2+}$ complex, the EPR line width decreases upon introduction of D_2O, showing an approximate 5.8 G decrease in the line width of the $-3/2$ perpendicular resonance feature with four equatorially located, inner-sphere-coordinated water molecules, i.e., 1.4 G decrease per water molecule (Mustafi & Makinen, 1988). For the solvated VO^{2+} ion in pure methanol, on the other hand, the decrease in EPR line width of the $-3/2$ perpendicular feature is about 3.6 G, i.e., 0.9 G decrease per methanol molecule. In pure methanol four equatorial positions can be occupied by the hydroxyl group of the methanol molecule. The smaller decrease of the EPR line width for the VO^{2+} ion in CD_3OD is consistent with the change in stoichiometry of protons of the equatorially coordinated hydroxyl groups (Mustafi & Makinen, 1988). The comparison of EPR line width of $[VO(H_2O)_5]^{2+}$ and $[VO(CH_3OH)_5]^{2+}$ complexes in natural abundance and deuterated solvents provides an important aspect concerning whether the equatorial ligands are water molecules or hydroxyl groups. Figure 5 illustrates the $-3/2$ perpendicular EPR feature of VO^{2+} ion complexed to NC-C in H_2O and D_2O. As illustrated in Figure 5, the decrease in line width of the $-3/2$ perpendicular EPR feature upon introduction of D_2O is approximately 2.4 G. In Table 2 we compare the line width of the $-3/2$ perpendicular EPR feature of $[VO(H_2O)_5]^{2+}$ and $[VO(CH_3OH)_5]^{2+}$ complexes and VO^{2+} complexes of NC-A and NC-C in H_2O and D_2O. As seen in Table 2, the EPR results of $VO^{2+}-$NC-C complexes are clearly different from that of $VO^{2+}-$NC-A complexes where no changes in line width were observed upon introduction of D_2O. Following the line width analysis of VO^{2+} complexes in natural abundance and deuterated solvents as in Table 2, these results indicate that, in the $VO^{2+}-$NC-C complex, it is most likely that there are two water molecules, not hydroxyl groups, directly coordinated to the VO^{2+} ion as equatorial ligands. Definitive proof of the inner-sphere coordinated water molecules relies on the ENDOR studies which are discussed below.

ENDOR can detect superhyperfine couplings of nearby nuclei with a greater sensitivity than EPR. For a system of low **g** anisotropy, as in the case of the VO^{2+} ion, proton ENDOR features appear symmetrically about the free nuclear Larmor frequency. Moreover, the axial character of the

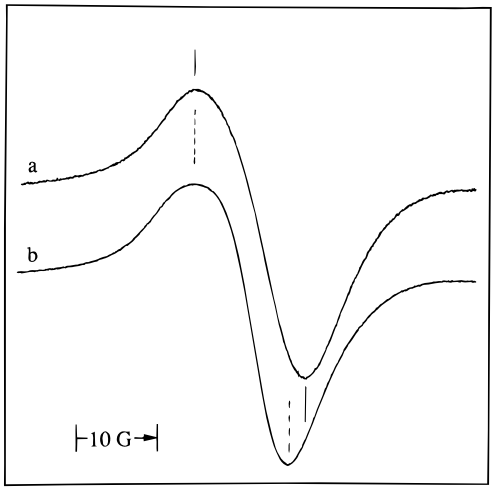

FIGURE 5: Comparison of the line width of the $-3/2$ perpendicular EPR feature for VO^{2+} ion complexed to NC-C: (a), in H_2O and (b), in D_2O. The solutions were buffered to pH 5.8 with 0.03 M PIPES. In both complexes $[VO^{2+}]$:[NC-C] molar ratios of 4:1 were used. The peak-to-peak line width for the $VO^{2+}-$NC-C complex in H_2O is indicated by solid lines, and the line width for the $VO^{2+}-$NC-C complex in D_2O is indicated by dashed lines.

Table 2: EPR Line Widths of VO^{2+} Complexes

	ΔH_{pp} (G)[a]		
complex	in protonated solvent	in deuterated solvent	ref[b]
$VO^{2+}-$pentaaquo	11.40	5.65	1
$VO^{2+}-$pentamethanol	9.78	6.16	1
$VO^{2+}-$NC-A	14.30	14.32	2
$VO^{2+}-$NC-C	13.70	11.33	this work

[a] The line width of $-3/2$ perpendicular EPR absorption feature was measured for each complex in natural abundance and perdeuterated solvents. [b] References: 1, Mustafi & Makinen, 1988; 2, Mustafi & Nakagawa, 1994.

vanadyl ion allows one to assign by ENDOR the spatial disposition of coordinating ligands as equatorial or axial (Mustafi & Makinen, 1988; Mustafi et al., 1992; Makinen & Mustafi, 1995). For purposes of discussing ENDOR results, a diagram is illustrated below that designates the direction of molecular axes with respect to the V═O bond.

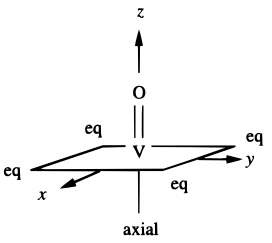

One axial position opposite to the V═O bond and four equatorial positions, labeled as eq, are also shown in the diagram. When $\mathbf{H}_0$ is applied to g_z (molecular *z* axis) at the low-field EPR absorption feature ($-^7/_2$ ||), $A_{||}$ of a proton located along the symmetry axis or $A_\perp$ of a proton located near or in the *x*,*y* plane should be observed. On the other hand, if $\mathbf{H}_0$ is set to an orientation perpendicular to g_z and, therefore, parallel to the *x*,*y* plane (i.e., $\mathbf{H}_0$ at $-^3/_2$ $\perp$), $A_\perp$ of a proton located along the symmetry axis and both $A_{||}$ and $A_\perp$ of a proton located near or in the *x*,*y* plane should be observed (Mustafi & Makinen, 1988; Makinen & Mustafi, 1995).

Figure 6 compares the proton ENDOR spectra of VO^{2+} complexed to NC-C with a metal:protein molar ratio of 4:1 in H_2O and D_2O, buffered to pH (or pD, pD = pH + 0.4) 5.8 with 0.03 M PIPES, to that of the pentaaquo oxovanadium ion. The well-resolved proton ENDOR features from protein residues in the vicinity of the VO^{2+} ion are seen in spectra a and b. For $[VO(H_2O)_5]^{2+}$, the proton ENDOR features of water molecules in the inner coordination sphere of VO^{2+} are indicated in the bottommost spectrum for both the axial and equatorial positions (Mustafi & Makinen, 1988). In the ENDOR spectrum of VO^{2+}−NC-C complex in H_2O (spectrum b), no proton resonance feature was observed that corresponded to axially bound water in the inner coordination sphere. At this magnetic field setting ($\mathbf{H}_0$ at $-^3/_2$ $\perp$ EPR feature), only perpendicular hfc components for axially located protons and both parallel and perpendicular hfc components for protons in equatorial positions should be observed. The line pair $a1_\perp$ was assigned to an axially located water proton that is located in the first coordination sphere, opposite to the V═O bond. The line pair $a2_\perp$ was assigned to another axially located water proton that is hydrogen-bonded to the vanadyl oxygen. On the other hand, in spectrum b two smaller line splittings, indicated by solid stick diagrams between the middle and the bottommost spectra, correspond very closely with ENDOR splittings of $e1_\perp$ and $e2_\perp$. In the pentaaquo oxovanadium ion, these line splittings, labeled as $e1_\perp$ and $e2_\perp$, were assigned as the perpendicular hfc components of the two classes of equatorially bound water molecules in the inner coordination sphere (Mustafi & Makinen, 1988). These features are not seen in spectrum a for the VO^{2+} ion complexed to NC-C in D_2O. Furthermore, for the VO^{2+}−NC-C complex in H_2O, two broad ENDOR features at about 20.7 and 21.5 MHz are observed, as illustrated in Figure 7. These resonance features are not seen for the VO^{2+} ion complexed to NC-A

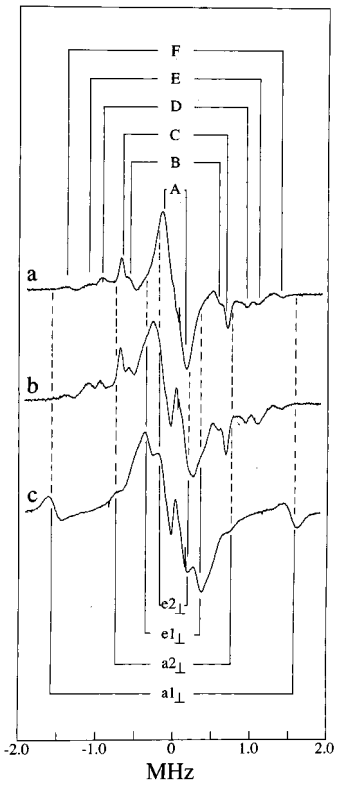

FIGURE 6: Proton ENDOR spectra of the VO^{2+} complexes in frozen aqueous solution. The magnetic field was set to $-^3/_2$ perpendicular EPR line at about 3264 G (see Figure 5). The spectra are shown for the following samples in top-to-bottom order: (a) VO^{2+}−NC-C complex (4:1 molar ratio of $[VO^{2+}]$:[NC-C]) in D_2O buffer; (b) VO^{2+}−NC-C complex (4:1 molar ratio of $[VO^{2+}]$:[NC-C]) in aqueous buffer; and (c) $[VO(H_2O)_5]^{2+}$ complex (VO^{2+} in H_2O/CD_3OH cosolvent mixture). Other conditions were as in Figure 3. The ENDOR line pairs are equally spaced about the free proton Larmor frequency of 13.9 MHz. The abscissa indicates the ENDOR shift (measured ENDOR frequency minus the free proton Larmor frequency). In spectrum c, proton ENDOR features from inner coordinated water molecules in the axial and equatorial positions, labeled as $a1_\perp$, $a2_\perp$ and $e1_\perp$, $e2_\perp$, respectively, are identified in the stick diagram with solid lines at the bottom. The ENDOR features $a1_\perp$ and $a2_\perp$ in spectrum c do not appear in spectra a and b, while the features labeled as $e1_\perp$ and $e2_\perp$ only appear in spectrum b, but not in spectrum a. The resonance features in spectrum c that are not seen in spectra a and b are indicated by dashed lines. The ENDOR line pairs in spectra a and b from protein residues, labeled as A−F, are indicated by the stick diagram with solid lines at the top.

in H_2O (lower spectrum in Figure 7). These two resonance features corresponding to larger hf couplings of 13.6 and 15.5 MHz are almost identical to those for the pentaaquo oxovanadium ion that were assigned to the parallel hfc components of the two equatorially bound water molecules (Mustafi & Makinen, 1988; van Willigen, 1980; van Willigen et al., 1982). These two resonance features are seen only in the ENDOR spectra with $\mathbf{H}_0$ at $-^3/_2$ $\perp$ EPR feature. The corresponding perpendicular hfc components of these two inner sphere, equatorially coordinated water molecules are seen in Figure 6, labeled as $e1_\perp$ and $e2_\perp$. As described by us previously, four equatorially bound water molecules in $[VO(H_2O)_5]^{2+}$ were classified into two groups and their positions were defined by the following: (i) equatorial hydroxyl protons of two water molecules lie exactly in the molecular *x*,*y* plane; and (ii) the hydroxyl protons for the other two water molecules lie below the molecular *x*,*y* plane (Mustafi & Makinen, 1988).

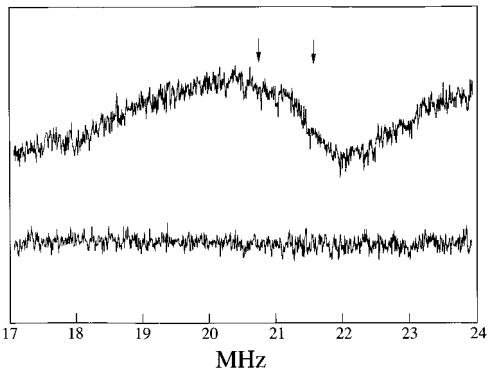

FIGURE 7: Proton ENDOR spectra of the VO^{2+} ion complexed to NC-C (upper spectrum) and to NC-A (lower spectrum) with $\mathbf{H}_0$ setting at the $-3/2$ perpendicular EPR line. In both complexes, metal: protein molar ratios of 4:1 were used in aqueous buffer. A modulation depth of 40 kHz of the rf field was employed. Other conditions were as in Figure 6. In the top spectrum of the VO^{2+} ion complexed to NC-C, two broad resonance features are indicated by arrows.

DISCUSSION

Comparison of Metal Binding Properties of NC-A and NC-C

We have carried out spectroscopic characterization of metal binding sites in both "strong" (NC-A) (Mustafi & Nakagawa, 1994) and "weak" (NC-C) inhibitor proteins. We have shown that VO^{2+} is an effective paramagnetic substitute for Ca^{2+} in both isoforms of NC. We have also demonstrated that VO^{2+} binds to both NC-A and NC-C with a stoichiometry of metal:protein binding of 4:1 and, most importantly, that VO^{2+} competes with Ca^{2+} in binding to both inhibitor proteins. However, CD studies revealed that conformational properties of proteins are different in NC-A and NC-C upon introduction of the native Ca^{2+} or VO^{2+}. For both VO^{2+} complexes of NC-A and NC-C, no ^{14}N-ENDOR feature is detected even at 4 K that could be attributed to a vanadyl-coordinated nitrogen-donor ligand. Furthermore, in both of these complexes, EPR parameters are compatible with only oxygen-donor ligands. However, the results of EPR and ENDOR studies of VO^{2+} complexed to NC-A and NC-C clearly indicate that the metal binding environment in "strong" and "weak" inhibitor proteins are different. In NC-C, the metal ion is exposed to solvent water molecules and two water molecules are detected by ENDOR in the inner coordination sphere of the metal ion. In the metal binding environment of NC-A, on the other hand, inner-sphere-coordinated water is completely excluded (Mustafi & Nakagawa, 1994).

On the basis of EPR and ENDOR spectroscopic studies, we have shown that NC-A differs from other known Ca^{2+}-binding proteins (Glusker, 1991; McPhalen et al., 1991), primarily because water is not retained in the inner coordination sphere of its metal binding sites. This observation is surprising because amino acid analysis shows a high content of Asp and Glu residues in kidney stone inhibitor proteins (Nakagawa et al., 1983, 1984, 1985a,b, 1987, 1991). Normally, one would assume that these negatively charged residues are hydrogen bonded to solvent molecules. In order to account for the exclusion of water molecules from the environment containing these ligands, we propose that Asp, Glu, and Gla residues favor oxygen-donor ligand−metal binding over hydrogen bonding to solvent molecules. The tight binding in NC-A is best explained by negatively charged carboxylate ions binding to metal ions in a hydrophobic environment. This can be rationalized when we consider that both Ca^{2+} and VO^{2+} exhibit very high affinity for binding to oxygen-donor ligands (Chasteen, 1981). Additional support of this hypothesis is provided by the fact that (i) NC-A exhibits tighter Ca^{2+}-binding affinity compared to other Ca^{2+}-binding proteins (Glusker, 1991; McPhalen et al., 1991), as expected if oxygen-donor ligands are involved in binding to Ca^{2+}; and (ii) VO^{2+} is coordinated only to oxygen-donor ligands in VO^{2+}−NC-A complexes (Mustafi & Nakagawa, 1994). In this respect, NC-A can be compared with the carp muscle Ca^{2+}-binding protein parvalbumin (Coffee & Bradshaw, 1973; Kretsinger & Nockolds, 1973). Parvalbumin contains two Ca^{2+}-binding sites, one of which is a high-affinity site with a dissociation constant of $<10^{-7}$ M, similar to that of NC-A (10^{-8} M). In this Ca^{2+}-binding site there are six oxygen-donor ligands from protein residues, and there is complete exclusion of inner-sphere water (Kretsinger & Nockolds, 1973). The tighter binding site in parvalbumin, with its highly charged residues located within a hydrophobic environment, favors metal binding (Yamashita et al., 1990). The strong binding of Ca^{2+} ions with oxygen-donor ligands in NC-A, as in parvalbumin, may provide a similar electrostatic environment for metal binding.

On the other hand, the metal binding environment in NC-C is found to be different than in NC-A, because in NC-C two water molecules are detected in the inner coordination sphere of the metal ion by EPR and ENDOR studies. This observation is unexpected because both inhibitor proteins contain a large amount of acidic, negatively charged amino acid residues Asp and Glu. One would assume that the metal binding environment in both types of inhibitor proteins is the same. However, NC-C, compared to NC-A, exhibits less affinity for metal binding. Other important distinctions between the strong and weak inhibitor proteins are (i) the weak inhibitor proteins are devoid of Gla residues; (ii) these two inhibitor proteins are different in their protein secondary structure of the polypeptide backbone; and (iii) unlike NC-A, NC-C shows no conformational change upon binding with metal ions. The weaker metal binding affinity in NC-C may provide an electrostatic environment that favors solvent molecules to bind with the metal ion, as seen in other Ca^{2+}-binding proteins that exhibit weaker affinity for metal binding (McPhalen et al., 1991). For NC-A, which exhibits much higher affinity for metal binding, it would be reasonable to expect considerable disruption of the local protein structure on removal of Ca^{2+}, as revealed by CD (Mustafi & Nakagawa, 1994). We believe that these differences, as outlined above, have an important bearing on the mechanism of inhibition of calcium oxalate monohydrate crystal growth by NC in renal tubules.

Possible Mechanism of Inhibition of COM Crystals by Nephrocalcin

The strong inhibitor protein (e.g., NC-A) has unique properties that prevent growth, aggregation, and secondary nucleation of COM crystals in renal tubules. NC-A shows a strong surface activity as expressed by an extremely high collapsing pressure of 41.5 dyn/cm, measured by a Lauda film balance, and shows a small limiting area per weight of the protein of 509 Å^2/molecule (Nakagawa et al., 1983, 1991). These properties indicate that the strong inhibitor

protein is very amphiphilic and has a highly organized structure at the air−water interface (Nakagawa et al., 1983). On the basis of kinetic studies using a seeded crystal growth system, Nakagawa et al. (1983) have shown that the inhibitor protein binds to the specific growth sites on COM crystal surface. They have also shown that, after binding to the surface of COM crystals, the strong inhibitor protein changes its conformation to an amphiphilic form with an elongated shape with an axial ratio of 1:6. The inhibitor protein forms a stable two-dimensional film that is able to cover a large area and binds to the surface of the COM crystals. As proposed by Nakagawa et al. (1983), the mechanism of inhibition of COM crystal growth by NC would involve the following steps. First, NC binds to the surface of COM crystals through negatively charged residues. Once anchored on the surface, the inhibitor protein assumes a secondary structure imposed by its asymmetric environment. The negatively charged residues of the inhibitor protein may recognize the particular crystal face of calcium oxalate. Thus, further crystal growth is inhibited by the hydrophobic moieties of the inhibitor protein exposed on the surface. These properties are lacking in the weak inhibitor protein, and, therefore, it cannot repress crystal growth.

The dissociation constant of weak inhibitor proteins (6×10^{-6} M) for binding COM crystals is about 2 orders of magnitude higher than that of the strong inhibitor proteins (4×10^{-8} M) (Nakagawa et al., 1983). The stronger binding affinity of COM crystals to NC-A may provide a situation that makes the growth of crystals, aggregation, and secondary nucleation processes kinetically unfavorable. We estimated that a normal adult excretes approximately 16 mg/L of the inhibitor protein, i.e., the concentration of NC is about 1.1×10^{-6} M. Since the concentration of NC is higher than the dissociation constant of NC-A for binding COM crystals, NC-A can efficiently inhibit crystal growth and aggregation at physiological concentrations. On the basis of our spectroscopic studies, we found that the strong inhibitor protein binds to Ca^{2+} (or COM crystals) through negatively charged residues, Asp, Glu, and Gla. Bernard et al., (1992) have recently shown on the basis of immunofluorescence experiments that human lithostathine, a pancreatic glycoprotein that inhibits the growth and nucleation of calcium carbonate crystals, binds to the surface of calcium carbonate crystals. Once NC-A binds to Ca^{2+} ions, a conformational change occurs as revealed by CD studies. In recent CD studies of metal-free NC-A with calcium oxalate crystals, we have found identical results to those of metal-free NC-A and $CaCl_2$. This indicates that NC-A binds to COM crystals similarly to Ca^{2+} ions. It is most likely that negatively charged carboxylate groups of the strong inhibitor protein recognize Ca^{2+} ions for metal binding and completely exclude water molecules from the metal binding environment, as revealed by EPR and ENDOR studies. The strong hydrophobic environment at the Ca^{2+}-binding sites or at the growth sites on the surface of COM crystals prevents further crystal growth and aggregation. The weak inhibitor protein (e.g., NC-C), on the other hand, does not change its conformation after binding to Ca^{2+} or COM crystals. It exhibits much weaker binding to COM crystals. Furthermore, the binding environment of NC-C at the COM crystal growth sites is much less amphiphilic. Thus, the electrostatic and solvent environments of NC-C at the crystal growth sites cannot prevent accumulation of calcium oxalate, allowing crystal growth to continue.

ACKNOWLEDGMENT

We thank Professor M.W. Makinen for helpful discussions and support.

REFERENCES

Ahmed, R. H., Nieves, J., Kim, L., Echegoyen, L., & Puett, D. (1987) *J. Protein Chem. 6*, 431−439.

Albanese, N. F., & Chasteen, N. D. (1978) *J. Phys. Chem. 82*, 910−914.

Ames, B. N. (1966) *Methods Enzymol. 8*, 115−118.

Bernard, J. P., Adrich, Z., Montalto, D., De Caro, A., De Reggi, M., Sarles, H., & Dagorn, J. C. (1992) *Gastroenterology 103*, 1277−1284.

Chasteen, N. D. (1981) in *Biological Magnetic Resonance* (Berliner, L. J., & Reuben, J., Eds.) vol. 3, pp 53−119, Plenum Press, New York.

Chasteen, N. D. (1983) *Struct. Bonding (Berlin) 53*, 105−138.

Chasteen, N. D., DeKoch, R. J., Roggers, B. L., & Hanna, M. W. (1973) *J. Am. Chem. Soc. 95*, 1301−1309.

Clamp, J. R., Bhatti, T., & Chamber, R. E. (1971) *Methods Biochem. Anal. 19*, 229−344.

Coffee, C. J., & Bradshaw, R. A. (1973) *J. Biol. Chem. 248*, 3305−3312.

DeKoch, R. J., West, D. J., Cannon, J. C., & Chasteen, N. D. (1974) *Biochemistry 13*, 4347−4354.

Francavilla, J., & Chasteen, N. D. (1975) *Inorg. Chem. 14*, 2860−2862.

Glusker, J. (1991) *Adv. Protein Chem. 42*, 1−76.

Kivelson, D., & Lee, S.-K. (1964) *J. Chem. Phys. 41*, 1896−1903.

Kretsinger, R. H., & Nockolds, C. E. (1973) *J. Biol. Chem. 248*, 3313−3326.

Makinen, M. W., & Mustafi, D. (1995) in *Metal Ions in Biological Systems* (Sigel, H., & Sigel, A., Eds.) Vol. 31, pp 89−127, Marcel Dekker, New York.

McPhalen, C. A., Strynadka, N. C. J., & James, M. N. G. (1991) *Adv. Protein Chem. 42*, 77−144.

Mustafi, D., & Makinen, M. W. (1988) *Inorg. Chem. 27*, 3360−3368.

Mustafi, D., & Nakagawa, Y. (1994*) Proc. Natl. Acad. Sci. U.S.A. 91*, 11323−11327.

Mustafi, D., & Makinen, M. W. (1995) *J. Am. Chem. Soc. 117*, 6739−6746.

Mustafi, D., Telser, J., & Makinen, M. W. (1992) *J. Am. Chem. Soc. 114*, 6219−6226.

Nakagawa, Y., Abram, V., Kezdy, F. J., Kaiser, E. T., & Coe, F. L. (1983) *J. Biol. Chem. 258*, 12594−12600.

Nakagawa, Y., Abram, V., & Coe, F. L. (1984) *Am. J. Physiol. 247*, F765−F772.

Nakagawa, Y., Abram, V., Parks, J. H., Lau, H. S.-H., Kawooya, J. K., & Coe, F. L. (1985a) *J. Clin. Invest. 76*, 1455−1462.

Nakagawa, Y., Otsuki, T., & Coe, F. L. (1985b) *FEBS Lett. 250*, 187−190.

Nakagawa, Y., Ahmed, M., Hall, S. L., Deganello, S., & Coe, F. L. (1987) *J. Clin. Invest. 79*, 1782−1787.

Nakagawa, Y., Renz, C. L., Ahmed, M., & Coe, F. L. (1991) *Am. J. Physiol. 260*, F243−F248.

Nancollas, G. H. (1979) *Adv. Colloid. Interface Sci. 10*, 215−252.

Robertson, W. G., Peacock, M., & Nordin, B. E. C. (1969) *Lancet 2*, 21−24.

van Willigen, H. (1980) *J. Magn. Reson. 39*, 37−46.

van Willigen, H., Mulks, C. F., & Atherton, N. M. (1982) *Inorg. Chem. 21*, 1708−1709.

Williams, R. J. P. (1985) *Eur. J. Biochem. 150*, 231−248.

Yamashita, M. M., Wesson, L., Eisenman, G., & Eisenberg, D. (1990) *Proc. Natl. Acad. Sci. U.S.A. 87*, 5648−5652.

BI961200J